

Rail Power Conditioner Based on Indirect AC/DC/AC Modular Multilevel Converter Using a Three-Phase V/V Power Transformer

Mohamed Tanta, José A. Afonso, *Member, IAENG*, António P. Martins,
Adriano S. Carvalho and João L. Afonso

Abstract—This paper presents a rail power conditioner (RPC) system based on an indirect AC/DC/AC modular multilevel converter (MMC) where a V/V power transformer is used to feed the main catenary line and the locomotives. The proposed control strategy for this system has been introduced to guarantee a good compensating performance of negative sequence currents (NSCs) and harmonics on the public grid side. This control strategy has also the ability to achieve balanced and equal voltage between the MMC's submodules (SMs) capacitors. Simulation results for this RPC based on an indirect MMC are presented in this paper to show the main advantages of using this topology. The results show how the proposed system is able to compensate NSCs and harmonics on the public grid side when the V/V power transformer feeds two unequal load sections.

Index Terms—modular multilevel converter (MMC), negative sequence currents (NSCs), rail power conditioner (RPC), submodules (SMs).

I. INTRODUCTION

The last decades have witnessed a rapid growth of high-speed and high power railways systems, with the appearing of new technologies to improve the efficiency and reduce the effects of AC railways traction grids on the power quality of the public grid side [1], especially when the railways traction grids are interconnected and have the same frequency of the public grid side (50 Hz), such as the case of Portugal and Finland. On the other hand, some countries, such as Germany and Austria, use different frequencies for the public grid (50 Hz) and the railway traction grid (16.7 Hz) [2]. The particular scopes of this paper are the harmonic distortion produced by the locomotives and the phase unbalance created by the single-phase traction loads [3].

Manuscript received in February 20, 2017; revised March 03, 2017. This work was supported by FCT (Fundação para a Ciência e a Tecnologia) with the reference project UID/EEA/04436/2013, COMPETE 2020 with the code POCI-01-0145-FEDER-006941.

Mohamed Tanta was supported by FCT grant with a reference PD/BD/127815/2016 and he is with GEPE (Group of Energy and Power Electronics) - Centro Algoritmi, University of Minho, Campus of Azurém, Guimarães, 4800-058, Portugal (e-mail: mtanta@dei.uminho.pt).

José Augusto Afonso is with CMEMS-UMinho (Center for Microelectromechanical Systems), University of Minho, Campus of Azurém, Guimarães, 4800-058, Portugal (phone: +351-253510190; fax: +351-253510189; e-mail: jose.afonso@dei.uminho.pt).

António Pina Martins is with SYSTEC (Research Center for Systems and Technologies), University of Porto, Rua Roberto Frias, 4200-465, Porto, Portugal. (e-mail: ajm@fe.up.pt).

Adriano da Silva Carvalho is with SYSTEC, University of Porto, Rua Roberto Frias, 4200-465, Porto, Portugal. (e-mail: asc@fe.up.pt).

João Luiz Afonso is with GEPE - Centro Algoritmi, University of Minho, Campus of Azurém, Guimarães, 4800-058, Portugal (e-mail: jla@dei.uminho.pt).

These matters are normally associated with the AC supply traction networks and they have been noticed from the early use of AC electrified railways. These drawbacks have the ability to create an adverse effect on the electric devices and threaten the safety and the economic operation of the high voltage public grids [1], [3].

Harmonic distortion in railway traction grids is mainly resultant from the electric locomotives and their old converter components, especially the old half controlled ones [1]. The second factor that affects the power quality is the unbalanced loads, which cause negative sequence currents (NSCs) [1], [4]. Eliminating the effects of NSCs requires to obtain a balanced load on public grid, and that is achievable by using different techniques, like static VAR compensators (SVCs) or static synchronous compensators (STATCOMs) [5].

The main disadvantage of SVCs is the production of harmonics, which are caused by the low switching frequency of power electronics devices [3]. Besides, a SVC may decrease the total power factor of the system when it is designed to compensate NSCs, because there is still a trade-off between power factor correction and NSCs compensation when using SVCs in railways traction systems [6]. STATCOM devices are used with medium voltage levels to compensate NSCs, and when this device is used in conjunction with a Scott transformer or a V/V transformer at the medium voltage levels of railways traction grid, it can be called as a rail power conditioner (RPC) [7].

Modular multilevel converters (MMCs) have been widely used with the medium voltage levels because of their flexibility and expandability to the required power value. Therefore, they have been enhanced recently to operate as RPCs in railways systems with different topologies, as in [8]–[10]. The RPC presented in [8] combines a direct AC/AC MMC and a Scott power transformer, while the one in [9] has the same direct AC/AC MMC but with a V/V power transformer. The RPC in [10] combines an indirect AC/DC/AC MMC and a Scott power transformer. Consequently, the direct AC/AC conversion with MMC requires to use full bridge submodules (SMs) that have positive, negative and zero output voltages, while the indirect AC/DC/AC conversion needs only half bridge SMs with only positive and zero output voltages [3].

This paper focuses on a RPC based on the indirect AC/DC/AC MMC with half bridge SMs and a V/V traction power transformer. This RPC system consists of a back-to-back single-phase MMC connected directly on parallel to the secondary side of a V/V power transformer and two load

sections, as shown in Fig. 1. This system is designed to compensate NSCs and harmonics on the public grid side.

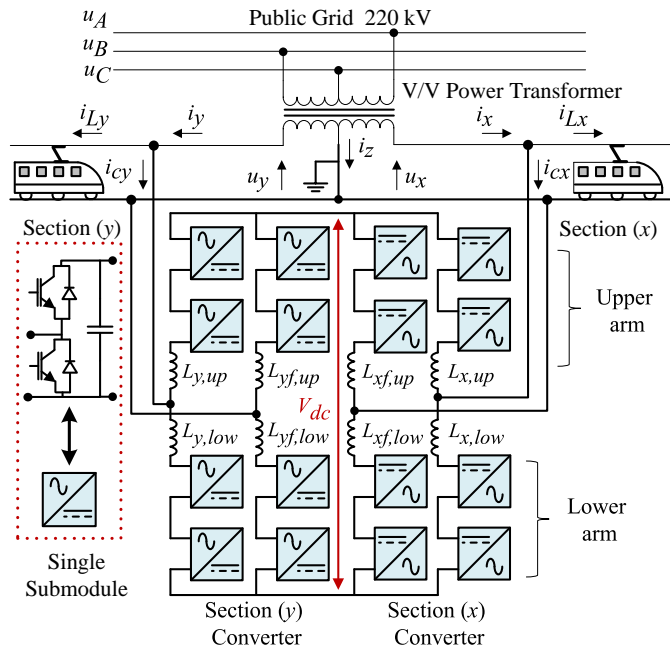


Fig. 1. RPC based on an indirect AC/DC/AC MMC connected to a V/V power transformer.

This paper has been organized as follows: Section II describes the RPC system in detail, Section III shows the operation principle with the control algorithm, Section IV provides the simulation results with different operation modes to validate the effectiveness of the system, and Section V summarizes the final conclusions of the work.

II. SYSTEM DESCRIPTION

A. Characteristics of the indirect MMC

This converter has the ability to be linked directly to medium voltage levels without using transformers and its structure depends on a cascade connection of half-bridge SMs. The DC-link of this converter has an inherent performance and is mainly formed from individual SMs capacitors. Therefore, there is no need to use a special DC-link capacitor like in a normal two-level back-to-back converter. Hence, capacitors voltage balancing control between SMs is important to guarantee a stable DC-link voltage [11]. The main motivations and features of using an indirect MMC with high and medium voltage levels are [12]:

- 1) Using a conventional two-level converter with high voltage levels requires to put a number of transistors in series to stand the desired voltage. This is unnecessary in a MMC, where normal transistors can be used because the high voltage will be divided between all SMs.
- 2) Small voltage steps in the output signals lead to less electromagnetic interference with other devices.
- 3) Multilevel voltage can reduce the harmonics distortion, so there is no need for filters on the AC grid side.
- 4) It is easy to increase the converter's power by adding more SMs.
- 5) There are less switching losses because of the low switching frequency for each SM.

A single-phase indirect MMC consists of two back-to-back converters and each converter connected directly to the catenary-ground lines of both load sections (x) and (y), as shown in Fig. 1. Each converter's leg has a coupled inductor, so the converter in all operates as a current source converter. Using the coupled inductor is very important to limit the current during voltage steps and to limit the circulating current between legs, especially after knowing that this current has high harmonics content, mainly the second harmonic; thus the inductances work like a converter's inner filter [12]. In addition, the coupled inductors are connected in series with SMs capacitors, so they have the ability to suppress any fault currents which could be resulting from the collapse of one or more capacitors [13].

B. Characteristics of the V/V power transformer

V/V transformers are commonly used in the high speed railway traction grids, because of reasons such as their simple structure, low price and high overload capability, when they compared with other power transformers [14].

It is very important to know that, without applying the compensation strategy of the RPC, and when an unbalanced V/V transformer is in use, the NSCs injected to the grid are half of the fundamental positive sequence when both load sections consume the same power. However, when a balanced transformer is in use (such as a Scott transformer or a Woodbridge transformer), no NSCs are injected to the public grid side when both load sections consume the same power [15], [6].

As a result and regardless to the used power transformer, equalization between two load sections is almost impossible in practical applications because the locomotives are operating asynchronously (e.g., one locomotive may be accelerating while another one is braking), and the RPC devices in such situations are required to compensate NSCs on the public grid side.

III. RPC OPERATION PRINCIPLE AND CONTROL ALGORITHM

A. Operation principle and mathematical analysis

By assuming that the power losses in the RPC power electronics devices are negligible, the main RPC operation principle is to shift half of the current difference of two load sections from the heavily loaded section to the lightly loaded one [15]. In the normal case, and without applying any compensation strategy, the voltages of two load sections u_x and u_y are in phase with the line voltages of u_{AC} and u_{BC} respectively. Consequently, and by considering a unity power factor, currents on public grid side are given by the equations (1), where K is the turns ratio of the V/V power transformer and $I_{Lx(rms)}, I_{Ly(rms)}$ are the RMS values of the two load sections currents.

$$\left. \begin{aligned} \dot{I}_A &= (I_{Lx(rms)} / K) e^{-j30} \\ \dot{I}_B &= (I_{Ly(rms)} / K) e^{-j90} \\ \dot{I}_C &= -(I_{Lx(rms)} / K) e^{-j30} - (I_{Ly(rms)} / K) e^{-j90} \end{aligned} \right\} \quad (1)$$

As in the RPC operation principle, the converter can shift half of the load currents difference, so the next equations could be applied [15].

$$\Delta I = \frac{1}{2}(I_{Lx(rms)} - I_{Ly(rms)}) \quad (2)$$

$$\left. \begin{aligned} \dot{I}_{A1} &= \dot{I}_A - \frac{\Delta I}{K} e^{-j30} = \frac{1}{2K}(I_{Lx(rms)} + I_{Ly(rms)})e^{-j30} \\ \dot{I}_{B1} &= \dot{I}_B + \frac{\Delta I}{K} e^{-j90} = \frac{1}{2K}(I_{Lx(rms)} + I_{Ly(rms)})e^{-j90} \end{aligned} \right\} (3)$$

Equations (3) show that phase A and phase B currents have now the same RMS value of:

$$I_{A1} = I_{B1} = \frac{1}{2K}(I_{Lx(rms)} + I_{Ly(rms)}) \quad (4)$$

Phase C does not, have the same RMS value that presented in equation (4) because the angles between phase A and phase B currents are not equal to 120°, as shown in Fig. 2(b). Moreover, phase C current is in phase now with its voltage, while the other two phases are still shifted by a 30° angle with the corresponded phase voltages because the reactive power is not compensated yet [14]–[16].

$$\left. \begin{aligned} I_{A1} &= I_{Lx} - \Delta I \\ I_{B1} &= I_{Ly} + \Delta I \\ I_{C1} &= \sqrt{3}I_{B1} = \sqrt{3}I_{A1} \end{aligned} \right\} (5)$$

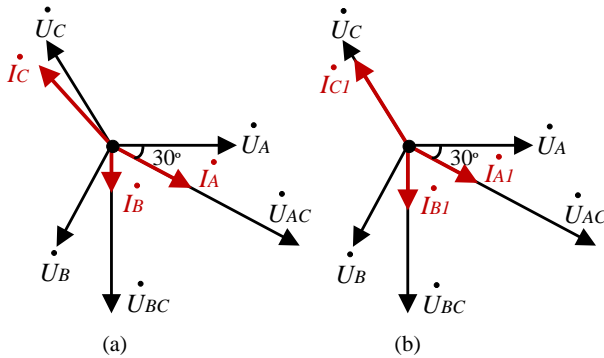


Fig. 2. Phasor diagrams of public grid currents: (a) When both load sections are loaded unequally without any compensation; (b) When shifting the active power difference.

In order to make the three-phase currents balanced, it is important to add a certain reactive current to phase x and phase y, as shown in Fig. 3. The RPC system has the responsibility of injecting the compensation currents i_{cx} and i_{cy} . Phase x generates reactive power because the reactive current component i_{cxr} that is injected by the section (x) converter leads the voltage vector of phase x. Phase y consumes reactive power because the reactive current component i_{cyr} that is absorbed by the section (y) converter lags the voltage vector of phase y, as shown in Fig. 3 (b). Furthermore, the phase currents on the public grid side i_{A2}, i_{B2}, i_{C2} have the same magnitude and are balanced [14].

From Fig. 3 (b) and equations (3), it is possible to obtain the following equations:

$$\left. \begin{aligned} I_{cxr} &= \frac{1}{2}(I_{Lx(rms)} + I_{Ly(rms)}) \tan \frac{\pi}{6} \\ I_{cyr} &= \frac{1}{2}(I_{Lx(rms)} + I_{Ly(rms)}) \tan \frac{\pi}{6} \\ \dot{I}_{x2} &= \dot{I}_{x1} + \dot{I}_{cxr} = \frac{1}{\sqrt{3}}(I_{Lx(rms)} + I_{Ly(rms)})e^{j0} \end{aligned} \right\} (6)$$

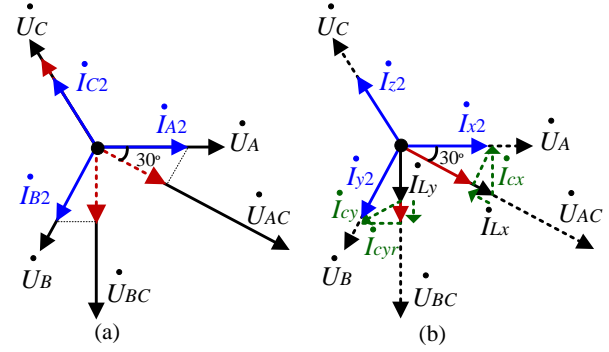


Fig. 3. Phasor diagram after shifting the active power difference and compensating the reactive power: (a) Public grid side; (b) Secondary side of the V/V power transformer.

Then, from the last equations of (6), the instantaneous values of currents after compensation are:

$$\left. \begin{aligned} i_{x2} &= \frac{\sqrt{2}}{\sqrt{3}}(I_{Lx(rms)} + I_{Ly(rms)}) \sin(\omega t + 0) \\ i_{y2} &= \frac{\sqrt{2}}{\sqrt{3}}(I_{Lx(rms)} + I_{Ly(rms)}) \sin\left(\omega t - \frac{2\pi}{3}\right) \\ i_{z2} &= \frac{\sqrt{2}}{\sqrt{3}}(I_{Lx(rms)} + I_{Ly(rms)}) \sin\left(\omega t + \frac{2\pi}{3}\right) \end{aligned} \right\} (7)$$

Equations (7) give the final balanced currents after shifting the active power difference between load sections and after compensating the reactive power [14] – [16].

B. Current control of the RPC

The control strategy of the RPC should inject the compensation currents of i_{cx} and i_{cy} . That is possible by calculating the reference values of i_{cx}^* and i_{cy}^* . In addition, the proposed control system should ensure a balanced voltage between all SMs capacitors of the MMC [12]. Compensation currents as reference signals contain the active and reactive components which should be generated by the RPC, and they can be obtained from Fig. 3 (b):

$$\left. \begin{aligned} i_{cx}^* &= i_{x2} - i_{Lx} \\ i_{cy}^* &= i_{y2} - i_{Ly} \end{aligned} \right\} (8)$$

The reference currents can be implemented by using the instantaneous load currents of the two load sections [15]:

$$\left. \begin{aligned} i_{Lx} &= \sqrt{2} \left(I_{Lxa} \sin\left(\omega t - \frac{\pi}{6}\right) + I_{Lxr} \sin\left(\omega t - \frac{2\pi}{3}\right) \right) + \sum_{h=2}^{\infty} i_{Lxh} \\ i_{Ly} &= \sqrt{2} \left(I_{Lya} \sin\left(\omega t - \frac{\pi}{2}\right) + I_{Lyr} \sin(\omega t - \pi) \right) + \sum_{h=2}^{\infty} i_{Lyh} \end{aligned} \right\} (9)$$

I_{Lxa}, I_{Lxr} are respectively the active and the reactive current components of load section (x). i_{Lxh} is the h^{th} -order of the instantaneous harmonic currents of load section (x). The same is applicable for $I_{Lya}, I_{Lyr}, i_{Lyh}$ of the load section (y). Then, by multiplying the equations (9) of i_{Lx} by $\sin(\omega t - \pi/6)$ and the equation of i_{Ly} by $\sin(\omega t - \pi/2)$, the results will contain DC components of $(\sqrt{2}/2)I_{Lxa}$ and $(\sqrt{2}/2)I_{Lya}$. Summing the DC components, then multiplying them by the value of $2/\sqrt{3}$, after filtering the signals by using a low pass filter, gives the peak value of phase x current after compensation, which has been presented in equations (7).

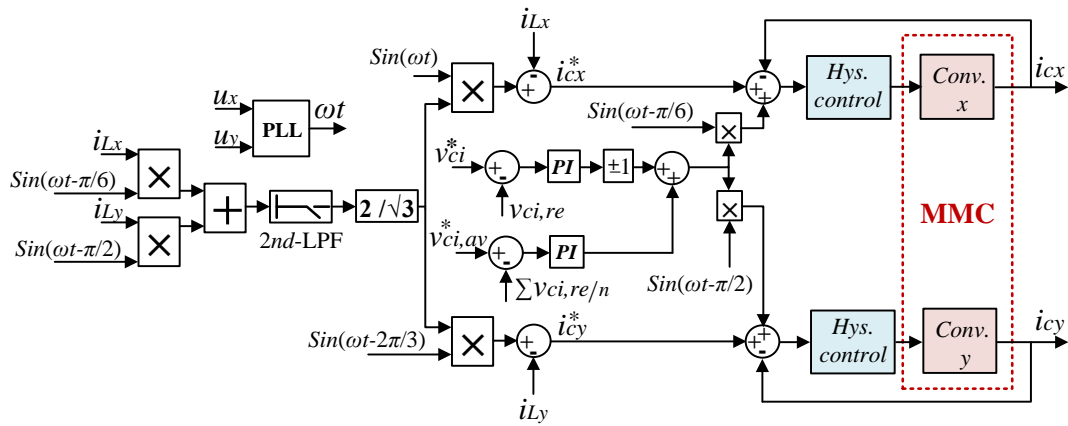


Fig. 4. Control strategy of the RPC based on an indirect MMC.

The previous assumption is only applicable after taking into consideration that the load power factor is almost one, because the locomotives normally use power converters, and in this case, locomotives currents contain mainly active components with harmonics [15], [17].

The total control topology of the RPC based on an indirect MMC, according to the previous equations, is shown in Fig. 4. The peak values of the phase x and phase y currents after compensation are equal. Therefore, it is possible to acquire the instantaneous values after multiplying them with the corresponded sine waves. Then, the reference compensation currents in equations (8) are calculated, and so the RPC has now the ability to compensate NSCs on the public grid side.

C. Capacitors voltage balancing control

To guarantee a good operation performance of the MMC, voltage balancing control for SMs capacitors must be applied to the system. This control consists of averaging voltage control and the individual voltage balancing control [11]. The averaging control ensures that the voltage of each capacitor in the leg is close to the average voltage that is provided as a reference. It is implemented by summing the measured capacitors voltages for each leg and dividing the result by the number of SMs per leg. The actual average voltage value in this case is calculated and compared to the reference average voltage value. Then, a proportional-integral controller (PI) is used to correct the difference between the actual and the reference values [12], [18].

The individual voltage balancing control is responsible to set every capacitor voltage to its reference. Therefore, another (PI) controller is used to correct the error and to act dynamically in the balancing process. The output of this controller is multiplied by 1 if the current's direction in the arm is to charge the capacitors, or by -1 if its direction is to discharge the capacitors. That is very useful to maintain a limited value for every SMs capacitor voltage [11], [12]. The next step is to have the instantaneous value for both signals of individual voltage balancing control and averaging control. That is possible by summing both signals and multiplying them by the corresponding sine waves of phase x and phase y [17]. The main function of the RPC is to track the reference currents of i_{cx}^* and i_{cy}^* , and that can be achieved by using a hysteresis controller for each converter on the

load section to ensure a fast response. The width of hysteresis controller H should have a suitable value. A large value of H causes low switching frequency and large tracking error, whereas a small value of H leads to high switching frequency but small tracking error [15].

IV. SIMULATION RESULTS

The simulation model has been built by using the *PSIM* software for power electronics simulation, in order to validate the system of RPC based on an indirect MMC and the associated control strategy. This simulation model consists of a 5-level indirect MMC with a total number of 32 SMs, and it is used for 25 kV, 50 Hz electrified traction grids. The main parameters of the simulation model are shown in Table I.

TABLE I
SIMULATION MODEL PARAMETERS

Parameters	Values
Public grid voltage	220 kV
Traction grid voltage	25 kV
Traction grid frequency	50 Hz
SM capacitance	100 mF
DC-link voltage	50 kV
Coupled inductor value	1 mH
Number of SMs in the leg (n)	8

As mentioned before, the load power factor on both load sections was considered to be close to one. Therefore, the locomotives can be modeled as a resistive load connected in parallel with an uncontrolled full bridge rectifier on the secondary side of the locomotive transformer. This full bridge rectifier is considered as a harmonic source, where the full locomotive model is shown in Fig. 5. The simulation results show two different case studies with much possible practical scenarios, when only one load section is loaded, and when both load sections are loaded unequally.

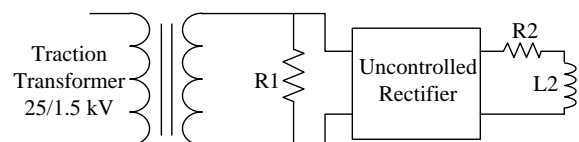


Fig. 5. Full locomotive model in *PSIM*.

A. Only one load section is loaded

By supposing that the load section (x) is loaded with 4.8 MW and section (y) is without any load, Fig. 6 (a) and Fig. 6 (b) show the waveforms of the public grid currents before and after applying the compensation strategy. The currents before compensation are totally unbalanced, and after the compensation they are balanced but with some harmonics contents due to a high value of the coupled inductance. Fig. 6 (c) shows the currents on the secondary side of the V/V power transformer.

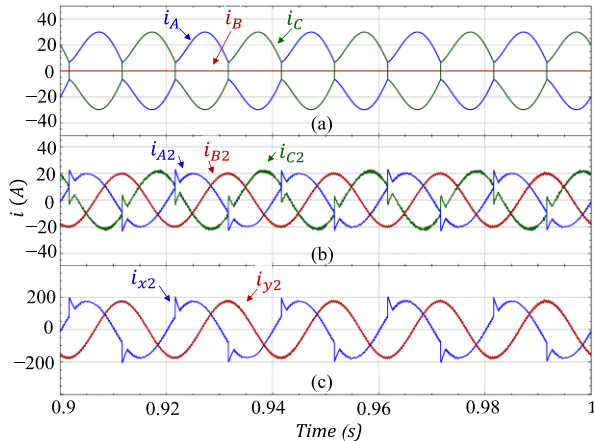


Fig. 6. Simulation results when section (x) is loaded: (a) Public grid currents before compensation; (b) Public grid currents after compensation; (c) Currents on the secondary of the V/V transformer after compensation.

Fig. 7 (a) shows the currents of both load sections, and it is clear that the section (x) current (locomotive current) has some harmonics contents. Fig. 7 (b) shows the compensation currents injected by the RPC. Current i_{cy} , which corresponds to the section (y) converter, is totally sinusoidal because the load section (y) is unloaded.

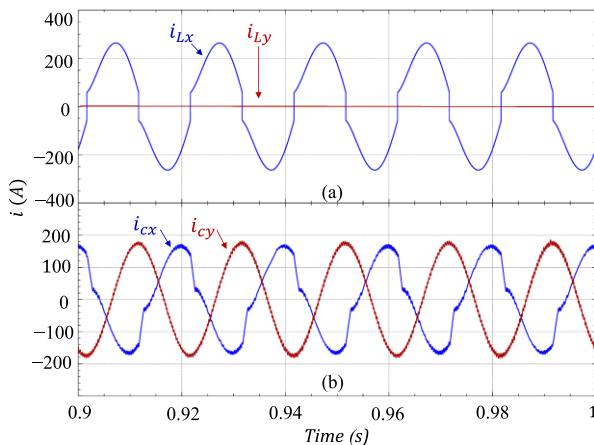


Fig. 7. Simulation results: (a) Load sections currents when only section (x) is loaded; (b) Compensation currents provided by the RPC.

Fig. 8 presents the waveforms of the SMs voltages and demonstrates the results of the applied voltage balancing control. Fig. 8 (a) shows the waveforms for the upper and the lower arms of the positive leg of section (x) converter. Fig. 8 (b) shows the same waveforms but for the negative leg of section (x) converter. Fig. 8 (c) shows the waveforms for the upper and the lower arms of the positive leg of section (y) converter. Fig. 8 (d) shows SMs voltages waveforms for the upper and the lower arms of the negative leg of section

(y) converter. The RPC control keeps the SMs voltages around their reference value of 13 kV.

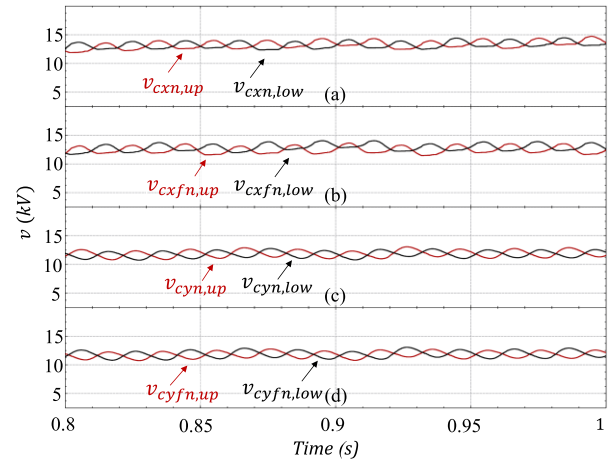


Fig. 8. SMs voltages when only section (x) is loaded: (a) SMs voltages of the positive leg of converter (x); (b) SMs voltages of the negative leg of converter (x); (c) SMs voltages of the positive leg of converter (y); (d) SMs voltages of the negative leg of converter (y).

B. Both load sections are loaded unequally

The second scenario is when both load sections are loaded unequally, the power of section (x) is 4.8 MW and the power of section (y) is 2.4 MW. The public grid side currents before applying the compensation strategy are presented in Fig. 9 (a) and they are unbalanced currents. Fig. 9 (b) shows the same currents after turning on the RPC. The public grid currents are now balanced, as shown in the phasor diagram of Fig. 3 (a). Fig. 9 (c) shows the currents on the secondary side of the V/V power transformer.

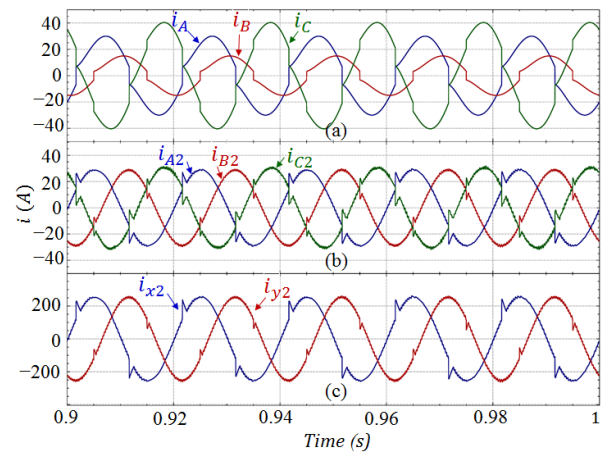


Fig. 9. Simulation results when both sections are loaded: (a) Public grid currents before compensation; (b) Public grid currents after compensation; (c) Currents on the secondary of the V/V transformer after compensation.

The load section currents are presented in Fig. 10 (a), where i_{Lx} has double of the value of i_{Ly} . Both currents are considered as harmonic sources because of using an uncontrolled rectifier in the locomotive model. The compensation currents that injected by the RPC are demonstrated in Fig. 10 (b), and i_{cy} here is not sinusoidal.

Similarly to Fig. 8, when only one load section was loaded, Fig. 11 shows the results of the applied voltage balancing control. Besides compensating the NSCs, the main aim of the RPC control is to maintain the SMs voltages around their reference value of 13 kV, as shown in Fig. 11.

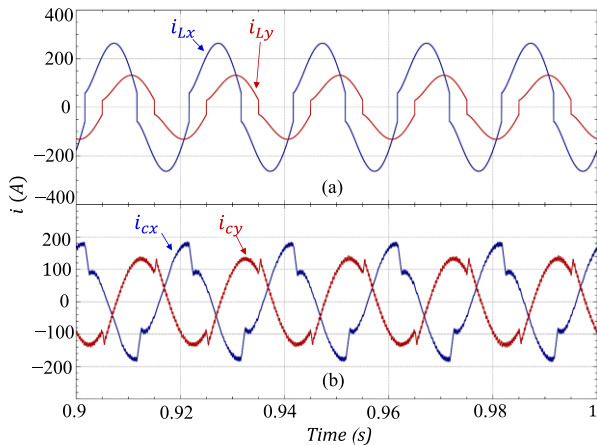


Fig. 10. Simulation results: (a) Load section currents when both sections are loaded unequally; (b) Compensation currents provided by the RPC.

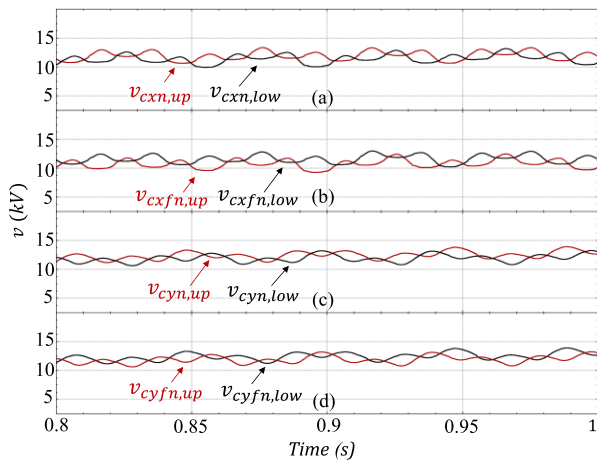


Fig. 11. SMs voltages when both sections are loaded: (a) SMs voltages of the positive leg of converter (x); (b) SMs voltages of the negative leg of converter (x); (c) SMs voltages of the positive leg of converter (y); (d) SMs voltages of the negative leg of converter (y).

V. CONCLUSION

This paper discussed a strategy to compensate negative sequence currents (NSCs) on the public grid side by using a rail power conditioner (RPC) based on an indirect modular multilevel converter (MMC) in AC electrified railways. Computer simulation using *PSIM* has confirmed the operation principle and the control strategy for the proposed system. The results showed balanced public grid currents in different operation scenarios. The RPC reference currents were generated depending on the load sections currents. In addition, voltage balancing control was added to ensure a constant DC-link voltage and equal voltage of submodules (SMs) capacitors. Nevertheless, SMs voltages waveforms when both load sections were loaded unequally had more fluctuations than the case when only one load section was loaded, and thus the control should be improved in the future by adding a circulating current controller for each MMC's leg.

REFERENCES

[1] I. Perin, P. F. Nussey, U. M. Cella, T. V. Tran, and G. R. Walker, "Application of power electronics in improving power quality and supply efficiency of AC traction networks," in *2015 IEEE 11th International Conference on Power Electronics and Drive Systems*, 2015, pp.1086–1094.

[2] A. Steimel, "Power-electronic grid supply of AC railway systems," in *2012 13th International Conference on Optimization of Electrical and Electronic Equipment (OPTIM)*, 2012, pp.16–25.

[3] I. Krastev, P. Tricoli, S. Hillmansen, and M. Chen, "Future of Electric Railways: Advanced Electrification Systems with Static Converters for ac Railways," *IEEE Electrification Mag.*, vol.4, no.3, pp.6–14, Sep. 2016.

[4] L. Abrahamsson, T. Schütte, and S. Östlund, "Use of converters for feeding of AC railways for all frequencies," *Energy Sustain. Dev.*, vol.16, no.3, pp.368–378, Sep. 2012.

[5] I. Perin, P. F. Nussey, T. V. Tran, U. M. Cella, and G. R. Walker, "Rail power conditioner technology in Australian Heavy Haul Railway: A case study," in *2015 IEEE PES Asia-Pacific Power and Energy Engineering Conference (APPEEC)*, 2015, pp1–5.

[6] C. Wu, A. Luo, J. Shen, F. J. Ma, and S. Peng, "A Negative Sequence Compensation Method Based on a Two-Phase Three-Wire Converter for a High-Speed Railway Traction Power Supply System," *IEEE Trans. Power Electron.*, vol.27, no.2, pp.706–717, Feb. 2012.

[7] S. Tamai, "Novel power electronics application in traction power supply system in Japan," in *2014 16th International Power Electronics and Motion Control Conference and Exposition*, 2014, pp.701–706.

[8] F. Ma, Z. He, Q. Xu, A. Luo, L. Zhou, and M. Li, "Multilevel Power Conditioner and its Model Predictive Control for Railway Traction System," *IEEE Trans. Ind. Electron.*, vol.63, no.11, pp.7275–7285, Nov. 2016.

[9] Q. Xu, F. Ma, Z. He, Y. Chen, J. M. Guerrero, A. Luo, Y. Li, Y. Yue, "Analysis and Comparison of Modular Railway Power Conditioner for High-Speed Railway Traction System," 2016.

[10] S. Song, J. Liu, S. Ouyang, and X. Chen, "A modular multilevel converter based Railway Power Conditioner for power balance and harmonic compensation in Scott railway traction system," in *2016 IEEE 8th International Power Electronics and Motion Control Conference (IPEMC-ECCE Asia)*, 2016, pp.2412–2416.

[11] M. Hagiwara and H. Akagi, "Control and Experiment of Pulsewidth-Modulated Modular Multilevel Converters," *IEEE Trans. Power Electron.*, vol.24, no.7, pp.1737–1746, Jul. 2009.

[12] A. Panagiotis, K. Papastergiou, M. Bongiorno, "Design and Control of Modular Multilevel Converter in an Active Front End Application," *Accelerators and Storage Rings -CERN; Engineering, Chalmers U. Tech, Gothenburg, Sweden*, 2013.

[13] Q. Tu, Z. Xu, H. Huang, and J. Zhang, "Parameter design principle of the arm inductor in modular multilevel converter based HVDC," in *2010 International Conference on Power System Technology*, 2010, pp.1–6.

[14] A. M. Bozorgi, M. S. Chayjani, R. M. Nejad, and M. Monfared, "Improved grid voltage sensorless control strategy for railway power conditioners," *IET Power Electron.*, vol.8, no.12, pp.2454–2461, Dec. 2015.

[15] A. Luo, C. Wu, J. Shen, Z. Shuai, and F. Ma, "Railway Static Power Conditioners for High-speed Train Traction Power Supply Systems Using Three-phase V/V Transformers," *IEEE Trans. Power Electron.*, vol.26, no.10, pp.2844–2856, Oct. 2011.

[16] F. Ma, A. Luo, X. Xu, H. Xiao, C. Wu, and W. Wang, "A Simplified Power Conditioner Based on Half-Bridge Converter for High-Speed Railway System," *IEEE Trans. Ind. Electron.*, vol.60, no.2, pp.728–738, Feb. 2013.

[17] V. P. Joseph and J. Thomas, "Power quality improvement of AC railway traction using railway static power conditioner a comparative study," in *2014 International Conference on Power Signals Control and Computations (EPSCICON)*, 2014, pp.1–6.

[18] M. Rejas, L. Mathe, P. Burlacu, H. Pereira, A. Sangwongwanich, M. Bongiorno, R. Teodorescu, "Performance comparison of phase shifted PWM and sorting method for modular multilevel converters," in *2015 17th European Conference on Power Electronics and Applications (EPE'15 ECCE-Europe)*, 2015, pp.1–10.